Article Category: New Results

Subject Area: Cancer Biology

TITLE:

SELECTIVE EPITHELIAL ACTIVATION OF KRAS^{G12D} DRIVES DUCTAL PANCREATIC NEOPLASIA IN SWINE

Carlos P. Jara[1], Al-Murtadha Al-Gahmi[1], and Mark A. Carlson[1,2]

1. Department of Surgery, University of Nebraska Medical Center, Omaha, Nebraska, USA
2. Department of Genetics, Cell Biology and Anatomy, University of Nebraska Medical Center, Omaha, Nebraska, USA

Carlos P. Jara (ORCID: 0000-0001-5444-721X)
Mark A. Carlson (ORCID: 0000-0002-8113-9199)

Corresponding author:

Mark A. Carlson
Department of Surgery
University of Nebraska Medical Center
983280 Nebraska Medical Center
Omaha, NE 68198-3280 USA
001-402-559-4581
macarlso@unmc.edu

ABSTRACT

Background: Pancreatic ductal adenocarcinoma (PDAC) remains a formidable challenge in oncology, characterized by a high mortality rate, largely attributable to delayed diagnosis and the intricacies of its tumor microenvironment. Innovations in modeling pancreatic epithelial transformation provide valuable insights into the pathogenesis and potential therapeutic strategies for PDAC.

Methods: We employed a porcine model, utilizing the Ad-K8-Cre adenoviral vector, to investigate the effects of variable doses (10^7 to 10^{10} pfu) on pancreatic epithelial cells. This vector, driven by a Keratin-8 promoter, delivers Cre-recombinase specifically to pancreatic epithelial cells. Intraductal pancreatic injections in transgenic Oncopigs (*LSL-KRAS*^{G12D}-*TP53*^{R167H}) were performed to evaluate epithelial cell proliferation and stromal response in a dose-dependent manner.

Results: Specificity of the adenoviral vector was validated through Keratin-8 expression and Cre-recombinase activity. We observed that the extent of macroscopic and histological alterations was dose-dependent. Higher doses resulted in significant tissue morphology changes, including atrophy and enlarged lymph nodes. Microscopic examination revealed concentration-dependent neoplastic transformation, characterized by ductal proliferation, cellular atypia, and stromal alterations. Notably, activation of the KRAS^{G12D} mutation corresponded with increased epithelial proliferation. Desmoplastic responses were evident through vimentin, α-SMA, and Masson's trichrome staining, indicating progressive collagen deposition, particularly at elevated viral titers.

Conclusion: Our study suggests a distinct dose-response relationship of Ad-K8-Cre in inducing pancreatic epithelial proliferation and neoplasia in an Oncopig model. While lower doses induced controlled epithelial proliferation, higher doses precipitated pronounced neoplastic and stromal alterations. These findings suggest the ability for precision in gene activation and high-light the potential to modulate the pancreatic tumor microenvironment in large animal preclinical models. The Oncopig model may emerge as an important tool in PDAC research, with clinically relevant pathology in a human-sized experimental model.

Keywords: PDAC, pancreatic cancer, Ad-K8-Cre, Oncopigs, neoplasia, desmoplastic reaction, KRAS^{G12D}

Author Approvals: all authors have seen and approved the manuscript, which has not been accepted or published elsewhere.

Competing Interests: The authors have declared no competing interest.

INTRODUCTION

Pancreatic ductal adenocarcinoma (PDAC) remains a challenge in public health, responsible for 7% of all cancer-related deaths. Furthermore, the patient prognosis is notably poor, with a five-year survival rate approximately at 9%, reflecting the disease's aggressive nature and challenges in treatment [1-3]. The use of large animal models, particularly porcine models, is changing our approach to PDAC research, leveraging their physiological and anatomical similarities to humans to overcome the limitations of traditional rodent models [4]. Porcine models are more significant due to their compatibility with standard human medical equipment [4]. This congruence accelerates the translation of new surgical and diagnostic techniques from experimental stages to clinical application [4]. The size of these models enables the replication of human interventional procedures, which are challenging to model in smaller animals, thus enhancing the clinical relevance of preclinical findings [4]. Furthermore, the porcine immune system, lifespan, and genomic characteristics closely mirror those of humans, playing a pivotal role in simulating the complex interactions within the human tumor microenvironment and in assessing long-term effects of therapeutic interventions [4].

The insidious onset of PDAC, where early stages are typically asymptomatic, presents significant challenges for detection and effective intervention. In our previous study we employed transgenic porcine model expressing the KRAS^G12D mutation [5], a prevalent oncogenic driver in PDAC, to elucidate the mechanisms of tumorigenesis and evaluate final-stage intervention strategies. The Cre-Recombinase dependent expression of this mutation allowed us for exploring of Pancreatic Cancer pathogenesis, offering insights into the initiation and progression of neoplastic transformations within the pancreas [5]. We used an adenovirus able to incorporate the Cre-Recombinase under the control of CMV promoter, allowing its expression in almost any cell type. In our new porcine model of ductal neoplasia, we explored the specific epithelial KRAS^G12D expression, as a novel platform for bridging the gap between early detection and treatment. Instead of CMV promoter, we employed Keratin 8 promoter, specific for epithelial cells. We believe by mirroring the gradual progression of human PDAC, this model could provide a useful platform to study early molecular events that could be targeted to halt or reverse the course of the disease. The gradient of neoplastic transformation observed in response to varied adenoviral vector concentrations could establish a framework for understanding the dose-dependent dynamics of oncogene activation and consequent tissue responses. The strategic employment of this porcine model holds the promise of transformative insights into PDAC, potentially enabling the development of interventions at a stage when the disease is most receptive to treatment, thus significantly altering the trajectory of this yet deadly disease.

RESULTS

KERATIN-8 AND CRE-RECOMBINASE EXPRESSION IN PANCREATIC CELLS

First, we explored Keratin-8 expression in pancreatic epithelial cells by using single-cell RNA sequencing from whole human pancreas. We successfully identified higher levels of Keratin-8 RNA expression in pancreatic ductal cells and acinar cells, both in human healthy and PDAC samples (Figure 1a). Also, we explored Keratin 8 staining in porcine pancreas. We identified epithelial cells (CAM5.2 staining) and Keratin 8 staining in accessory and main duct in both wild type and Oncopig pancreas (Figure 1b). Then, we performed an e*x vivo* assessment of the Ad-K8-Cre Adenovirus (a vector construct with Keratin 8 promoter driving the expression of the Cre-Recombinase) in wildtype porcine pancreas (Figure 1c, Supplementary S1a). This *ex vivo* infection assay showed that the expression of Cre-recombinase under the control of the Keratin 8 promoter was limited to the epithelial cells, confirming the selective activity of the adenoviral construct in pancreatic epithelial cells (Figure 1d).

EFFECTIVE INTRADUCTAL INJECTION PROCEDURE SHOWED MACROSCOPIC ALTERATIONS AFTER DOSE-RESPONSE IN ONCOPIGS

After confirming the target expression of Cre-recombinase by Ad-K8-Cre in pancreatic epithelial cells, we evaluated the target epithelial activity of Ad-K8-Cre adenovirus in vivo (Supplementary S1b). We injected (intraductal pancreatic injections) Ad-K8-Cre adenovirus at different concentrations (ranging from 10^7 to 10^10 pfu) in eight transgenic Oncopigs (Figure 2a,b). Briefly, our laparotomy procedure initiated with an incision below the xiphoid extended to the past umbilicus in females and approached the urethral meatus in males. The dissection progressed through subcutaneous fat, fascia, and muscle layers, ultimately reaching the pre-peritoneal space via electrocautery. After retracting the small and large bowel caudally, the stomach's pyloric region was brought into view. This process facilitated the expose of the duodenal segment of the pancreas (Figure 2a,b). Notably, a distinct window between the connecting-lobe of the pancreas, duodenum, and pancreatic head was established. Using surgical loupes (with 3.5x magnification), the pancreatic duct located within the duodenal side of the connecting lobe became identifiable. Upon successful cannulation (from connective lobe to pancreatic head) using a 22G angiocath, the specified concentration of Ad-K8-Cre (from 10^7 to 10^10 pfu) in 100-150uL was administered into the pancreatic duct (Figure 2c). After 2 months post-injection, all Oncopigs survived (Table 1).

After 2 months, Oncopigs injected with doses ranging from 10^9 to 10^10 pfu presented a distinct appearance (Figure 3a). The injection site exhibited a fragmented morphology characterized by multiple tissue clusters with enlarged reactive lymph nodes present around the pancreas (Figure 3a-c). Notably, the coloration was paler (or *icteric*) than the control, or other adenoviral concentrations, and the pancreas exhibited signs of atrophy (Figure 3a, d). On the other hand, Oncopigs injected with doses ranging from 10^7 to 10^8 pfu showed conserved morphology of the pancreas. At the macroscopic level, the injection site showed neither tangible damage nor significant pathological alterations. While there were lymph nodes present around the pancreas as well, there was an absence of discernible masses or marked discoloration to suggest atypical growth or inflammation (Figure 3b,c). Also, weight, hemoglobin (HG), hematocrit (HCT), amylase, lipase, carcinoembryonic antigen (CEA), CA 19-9, and alpha-fetoprotein (AFP) showed no significant changes post-injection with Ad-K8-Cre across different dosage groups, indicating that the selective epithelial activation of KRAS^G12D mutation had minimal systemic impact on these parameters (Table 1, Table 2).

EPITHELIAL KRAS^{G12D} ACTIVATION DRIVES NEOPLASTIC CHANGES

After 2 months post Ad-K8-Cre delivery, histological examination of pancreatic samples exhibited signs of cellular changes associated with neoplastic transformation. This transformation was observed as we noted an increase in architectural disruption and cellular irregularities from the 10^7 to the 10^10 pfu concentrations (Figure 4a). We found distinct differences in tissue architecture between the injection and non-injection sites, especially at the highest Ad-K8-Cre concentrations (Figure 4a). Also, we found cellular atypia, characterized by an irregular arrangement of ductal cells and nuclear changes, accentuated in the 10^9 and 10^10 concentration compared to those injected with 10^7 (Figure 4a). Notably, Oncopigs injected at higher concentration displayed more pronounced signs of complex ductal proliferation and cellular atypia when compared to those injected with lower adenoviral concentrations. These ductal structures were formed by dense Ki67-positive neoplastic cells, evident at any Ad-K8-Cre concentrations tested (Figure 4b). While the 10^7 to 10^9 pfu concentrations display a ductal proliferation pattern, the 10^10 pfu showed a loss of distinct circular or ovoid proliferation areas, with stronger, more dispersed, and homogenous staining pattern throughout the sample. Then, we suggest a dose-dependent neoplastic response to Ad-K8-Cre administration. On the other hand, non-injection sites consistently maintained tissue homogeneity. These samples displayed uniform tissue structures and quiescent Ki67 pattern (Figure 4a-b). We suggest such changes in the Oncopigs were potentially attributable to the activation of the KRAS^{G12D} and P53^{R167H} mutations in pancreatic epithelial cells under the control of the epithelial-dependent Cre-recombinase expression. To validate this, we needed to demonstrate two key events: the targeted KRAS^{G12D} expression within neoplastic cells, and the positivity of these cells for epithelial markers.

Targeted KRAS^{G12D} expression within Neoplastic Cells. After 2 months post Ad-K8-Cre injection, we observed a target induction of the KRAS^{G12D} expression within neoplastic cells. Sections from the Ad-K8-Cre-injected samples demonstrated a pronounced KRAS^{G12D} expression (Figure 5a). These staining patterns were particularly evident in the areas with disrupted architecture and complex ductal proliferation, aligning with our earlier observations of neoplastic transformation. This staining corroborates that the Ad-K8-Cre delivery was successful in inducing targeted KRAS^{G12D} expression within the transformed cells. Interestingly, regions that tested positive for the KRAS^{G12D} mutation also displayed a corresponding rise in Ki-67 expression. This underscores the quiescent nature of the healthy pancreatic cells (Fig 4b, Fig 5a) compared to the aggressive growth pattern observed in the neoplastic tissue.

Cytokeratin expression in ductal neoplasia suggest epithelial origin. Continuing, we turned our focus towards the epithelial markers, specifically CAM5.2 and Cytokeratin 7, to explore the epithelial nature of these neoplastic cells post transformation. CAM5.2 (Figure 5b) and Cytokeratin 7 (Supplementary S2a) staining revealed a pronounced expression of the markers across all injected pancreases. We observed the highest staining intensity in samples from Oncopigs injected within 10^9 and 10^10 concentrations, highlighting the effectiveness at elevated doses. On the other hand, the epithelial marker was reduced in non-injected samples, emphasizing the precision of the Ad-K8-Cre delivery, and suggesting the maintained epithelial lineage post-transformation. This, contrasting with the healthy porcine pancreas, which demonstrated strong, consistent throughout the ductal cells.

DUCTAL NEOPLASIA IS ACCOMPANIED BY PROGRESSIVE DESMOPLASTIC CHANGES AND COLLAGEN DEPOSITION

The histological features of pancreatic ductal neoplasia and associated stromal changes were systematically characterized through vimentin, α-SMA, and Masson's trichrome staining (Figure 6a-c).

We found distinct desmoplastic changes with increased collagen deposition (Figure 6a). At the 10^7 concentration (Figure 6a), there was an increase in collagen deposition at the injection site compared to the non-injection site, with mild desmoplastic reaction. At the 10^8 concentration (Figure 6a), the stroma displayed a moderate increase in collagen deposition, potentially associated with a more aggressive neoplastic behavior. At the 10^9 concentration, we found enhanced desmoplastic response. The collagen deposition was marked by a dense blue staining, suggesting a substantial fibrotic reaction within the pancreatic stroma. At the highest concentration of 10^10, the Masson's trichrome stain showed a robust desmoplastic reaction (Figure 6a). The intense staining indicates extensive collagen deposition and suggest a dose-dependent desmoplastic reaction, with increased concentrations leading to more pronounced fibrosis. Additionally, we examined the stromal alterations via α-SMA immunohistochemistry (Figure 6b). We observed a concentration-dependent intensification of α-SMA positivity, signifying a proliferative stromal reaction at the sites of injection. This was markedly pronounced at the highest viral titers, indicative of a potentiated desmoplastic response in the vicinity of neoplastic ductal clusters. Conversely, α-SMA expression remained marginal within non-injected pancreatic tissue (Figure 6b). We found increased vimentin positivity within the stroma surrounding the neoplastic ductal cells, characteristic of desmoplastic reaction (Figure 6c). The 10^9 to 10^10 pfu concentrations showed the most intense and widespread staining due to the pronounced desmoplastic changes observed, correlated with the increased neoplastic activity, as evidenced by collagen deposition and α-SMA staining.

In comparison, the examination of Human Pancreatic Cancer samples (Supplementary S3) showed a distinct advancement in neoplastic transformation. These samples demonstrate considerable architectural disruption, indicative of the disease's advanced progression. The human samples were characterized by enhanced desmoplastic reactions and increased collagen deposition, which were more pronounced compared to the early-stage changes observed in the Oncopig model.

Collectively, these histopathological findings delineate a clear dose-response relationship between the injected Ad-K8-Cre and the resulting stromal changes. The data underscore the dynamic interplay between neoplastic ductal cells and their microenvironment.

NEOPLASTIC CLUSTERS SUGGESTED AN INCREASED PRODUCTION OF MUCIN

We found acidic mucins within the ductal epithelium and stroma, with an increasing gradient in response to the rising concentrations. The spatial distribution of these stains highlighted the aberrant mucin production pattern compared to healthy pancreatic tissue. In contrast to the neoplastic tissue, healthy samples displayed minimal blue or magenta staining, underscoring the nominal presence of mucin in normal pancreatic cells (Figure 7a).

CONCLUSION

The utilization of larger animal models such as pigs provides distinct advantages over traditional rodent models in the study of pancreatic ductal adenocarcinoma (PDAC). These models' size allows for the use of standard human diagnostic and therapeutic equipment, facilitating clinically relevant simulations, particularly for procedures like surgical and interventional radiology techniques that are not easily replicated in smaller models [6]. Furthermore, the porcine model's immune system, lifespan, and genetic makeup are more closely aligned with humans, providing a biologically accurate context for studying complex diseases like PDAC [7]. This similarity is especially beneficial for understanding the human-like tumor microenvironment's critical role in tumor progression and response to therapy [8].

The targeted expression of the KRAS^G12D mutation within our porcine model underscores the potential of large animal models to advance our understanding of PDAC pathogenesis. This approach could facilitate the detailed observation of neoplastic transformation and early intervention studies, which could significantly impact survival outcomes [9]. Our model may provide a powerful platform for preclinical assessment of novel therapeutics and diagnostics, potentially improving the predictability of clinical trial outcomes and accelerating effective treatment development [10].

Our study demonstrates that intraductal administration of the adenoviral vector Ad-K8-Cre induces a dose-dependent effect on epithelial cell proliferation and stromal reactions within pancreatic tissue. We believe an important finding is the dose-related correlation between Ad-K8-Cre concentrations and the selective proliferation of epithelial cells harboring the KRAS^G12D mutation, a known oncogenic driver in pancreatic neoplasia.

The potential of our model extends to illuminating the crucial transition from pre-neoplastic to overtly neoplastic states. Identifying and understanding these early transitions could pave the way for timely interventions, potentially altering the disease's course [15]. The implications of such research include the possibility of developing targeted therapies that could disrupt pancreatic cancer at its inception or in its early course, changing the trajectory of this lethal disease[16]. With recent progress in pancreatic imaging, it is likely that a trend to earlier diagnosis of pancreatic cancer will progress. This raises the possibility for less invasive and less morbid procedures that could be used to ablate pancreatic cancer. An early-stage large animal PDAC model such as described in this manuscript could facilitate the development of such less invasive therapeutic modalities.

At a lower concentration (10^7), Ad-K8-Cre promotes epithelial proliferation while preserving the structural integrity of ductal formations. This suggests that the adenoviral vector can precisely target and stimulate the proliferation of epithelial cells with the active KRAS^G12D mutation without disrupting the ductal architecture. Moreover, this concentration initiates a mild desmoplastic response, evident from the increase in collagen deposition and α-SMA expression, indicative of an early stromal activation.

In contrast, the highest concentration tested (10^10) leads to a marked increase in disorganized epithelial proliferation, as evidenced by diffuse Ki67 staining, and a robust desmoplastic reaction characterized by extensive collagen deposition and α-SMA expression. This suggests that at elevated concentrations, Ad-K8-Cre not only impacts epithelial cells but may also affect the surrounding stroma, triggering an aggressive fibrotic response that could potentially modify the tumor microenvironment and influence neoplastic behavior.

The findings suggest that while lower concentrations of Ad-K8-Cre offer a targeted proliferative stimulus, potentially useful for therapeutic interventions, higher concentrations may disrupt tissue homeostasis, precipitating unregulated growth and significant stromal changes. These insights highlight

the importance of dosage precision in mutant gene activation aiming to manipulate oncogenic pathways and stromal dynamics within the pancreatic tumor microenvironment.

[The following section may be included in the final draft]

Our technique for inoculating the Oncopig pancreatic duct[5] ensures targeted delivery of the adenoviral vector Ad-K8-Cre. This method contrasts with traditional systemic or parenchymal delivery methods, which often result in less specific targeting and variable efficacy. The precision of our intraductal injection technique ensures that the adenovirus directly reaches the pancreatic epithelial cells, maximizing the potential for targeted gene activation. Our study's results demonstrate the effectiveness of this technique, as evidenced by the successful expression of Cre-recombinase in pancreatic epithelial cells following intraductal administration of the Ad-K8-Cre adenovirus. This successful targeting is crucial, given that KRAS mutations, specifically epithelial KRAS^G12D expression, play a pivotal role in the pathogenesis of PDAC and are a key focus of therapeutic interventions.

While similar approaches have been attempted, such as endoscopic retrograde cholangiopancreatography (ERCP)-based methods for gene delivery, these techniques often present challenges in terms of accessibility and precision (Yamaguchi et al., 2020). Our laparotomy-based approach, involving detailed anatomical dissection and direct visualization of the pancreatic duct, allows for a more controlled and precise delivery, potentially overcoming the limitations faced by other methods. However, it does require major surgery (i.e., open entry into a body cavity).

METHODS

Surgical Procedure

All Oncopigs underwent Tumor indirection in the same fashion. The Oncopigs were pre- anesthetized using an intramuscular injection of Telazol®-Ketamine-Xylazine and taken to the Operating Room. They were placed in the supine position, intubated with 6-7 French endotracheal tube, and maintained on continuous Isoflurane inhalation. Vitals were monitored noninvasively and maintenance fluid, Lactated ringers' solution, was given throughout the case.

Skin was shaved and prepped with chlorohexidine, weight-based bupivacaine was administered locally over the upper abdominal midline, and abdomen was draped in sterile fashion. An incision was made below the xiphoid extending down past umbilicus in females and proximal to the urethral meatus in males with #10 blade. This was then carried down through subcutaneous fat, facia and muscle to the pre-peritoneal space using Electrocautery.

The peritoneum was carefully incised to enter the greater sac and a Bookwalter retractor was assembled and used to provide adequate abdominal exposure. The small and large bowel was retracted caudally, and the stomach grasped at the Pylorus brought out into view and reflected Antero-superiorly and caudally, as needed, to expose the duodenal segment of the pancreas. Pancreatic adhesions to small/large bowels were lysed and a window between the connecting-lobe of the pancreas, duodenum and pancreatic head was created and isolated with silk suture.

The proximal part of the connecting-lobe of pancreas was tied with 2-0 silk and transected 0.5-1cm from its origin on the pancreatic head. With the aid of surgical loupes (3.5x the optical zoom) the pancreatic duct in the distal connecting lobe was identified and cannulated with 22g Angiocath; the injectate with the desired concentration of AdCre was injected into the pancreatic duct and the distal connecting lobe of pancreas was tied with 2-0 silk suture.

Final inspection and hemostasis were performed, and skin and tissue were then closed in the following fashion: The peritoneum was reapproximated with 3-0 Vicryl suture, abdominal fascia with 0-Maxon suture, Scarpa's fascia with 4-0 Vicryl suture, and then the dermis with 4-0 Vicryl suture. Dermabond adhesive glue was then placed over the incision. The Oncopigs were extubated after confirmation of spontaneous breathing and continued to be monitored until O2 saturations remined greater than > 90 without need for oxygen.

Post-operatively, the swine were housed in individual pens until day 4 in order to prevent wound cannibalism, after which they were regrouped with their respective sex. All animals were monitored for recovery for 3 days postoperatively and kept NPO until day 2. Once clinically stable, feeding was reinitiated. The swine contained to be assessed for signs of deterioration until the planned euthanasia date.

At 2 months post AdCre induction, the Oncopigs underwent necropsy. Anesthesia and access to the abdomen was obtained in a similar fashion taking care to lyse adhesions and avoid bowel injury. The diaphragm was then accessed below xiphoid and extended on either side to expose the IVC and the Oncopigs were euthanized with weight based Fatal-Plus (1mL/10 lb body wt) injected into the IVC followed by palpation of heart to confirm cessation of cardiac activity, and then complete transection of the IVC. The pancreas and surrounding tissue then underwent gross evaluation and circumferential excision with tissue specimens collected from the injection site (connecting lobe), non-injection site (tail of pancreas) and lymph nodes for histopathologic analysis.

Ex Vivo Porcine Pancreatic Main Duct Analysis

Porcine pancreases were harvested from wild type domestic pigs. The main pancreatic duct was carefully isolated from the harvested pancreas. The isolated pancreatic main duct was meticulously chopped into small pieces. The dissected pancreatic duct pieces were placed in a 6-well plate. Each well was filled with DMEM supplemented with 10% FBS (tetracycline-free). A dose of 10^9 pfu of Ad-K8-Cre was added to each well. The plate was incubated overnight in a 5% CO2 incubator. Following incubation, the samples were fixed using 4% paraformaldehyde overnight. The fixed samples were then embedded in paraffin and sectioned at 5µm thickness. The sections were incubated overnight with an anti-recombinase antibody. Post incubation, the sections were stained using DAB to visualize the recombinase expression.

Immunohistochemistry and Histological

Tissue Harvesting. Following the dose-response in vivo experiment, pancreatic tissues were harvested from porcine subjects. Two distinct samples were obtained from each subject: Injection Site (Connective lobe where AdCre was administered) and non-injection Site (Area distant from the injection site, particularly the tail or splenic lobe of the pancreas)

Fixation and Sectioning. Harvested samples were immediately fixed in cold 4% paraformaldehyde overnight. Post-fixation, the tissues were embedded in paraffin and serially sectioned at 5µm thickness. Three serial sections from both regions (injection and non-injection sites) per animal were prepared for IHC and histological analysis.

Immunohistochemical Staining. The tissue sections were incubated overnight with the following primary antibodies: Anti-cytokeratin 8, Anti-cam5.2 Anti-KRAS G12D, Anti-Ki67, and Anti-cadherin. After incubation, the sections were treated with DAB to detect protein expression.

Histological Staining. [this section to be completed] Hematoxylin and Eosin (H&E): To assess general tissue morphology.

Masson Trichrome: To visualize collagen and muscle fibers.

Alcian blue-Periodic Acid Schiff (PAS): To identify mucins and polysaccharides in the tissue.

All staining procedures were carried out in accordance with manufacturer's recommendations.

REFERENCES

1. Yu Y, Yang G, Huang H, Fu Z, Cao Z, Zheng L, et al. Preclinical models of pancreatic ductal adenocarcinoma: challenges and opportunities in the era of precision medicine. Journal of Experimental & Clinical Cancer Research. 2021;40(1):8.
2. Sarantis P, Koustas E, Papadimitropoulou A, Papavassiliou AG, Karamouzis MV. Pancreatic ductal adenocarcinoma: Treatment hurdles, tumor microenvironment and immunotherapy. World J Gastrointest Oncol. 2020;12(2):173-81.
3. Orth M, Metzger P, Gerum S, Mayerle J, Schneider G, Belka C, et al. Pancreatic ductal adenocarcinoma: biological hallmarks, current status, and future perspectives of combined modality treatment approaches. Radiation Oncology. 2019;14(1):141.
4. Bailey KL, Carlson MA. Porcine Models of Pancreatic Cancer. Front Oncol. 2019;9:144.
5. Mondal P, Patel NS, Bailey K, Aravind S, Cartwright SB, Hollingsworth MA, et al. Induction of pancreatic neoplasia in the KRAS/TP53 Oncopig. Disease models & mechanisms. 2023;16(1).
6. Sieren JC, Meyerholz DK, Wang XJ, Davis BT, Newell JD, Jr., Hammond E, et al. Development and translational imaging of a TP53 porcine tumorigenesis model. The Journal of clinical investigation. 2014;124(9):4052-66.
7. Leach SD. Mouse models of pancreatic cancer: the fur is finally flying! Cancer Cell. 2004;5(1):7-11.
8. Hezel AF, Kimmelman AC, Stanger BZ, Bardeesy N, Depinho RA. Genetics and biology of pancreatic ductal adenocarcinoma. Genes & development. 2006;20(10):1218-49.
9. Hingorani SR, Petricoin EF, Maitra A, Rajapakse V, King C, Jacobetz MA, et al. Preinvasive and invasive ductal pancreatic cancer and its early detection in the mouse. Cancer Cell. 2003;4(6):437-50.
10. Morton JP, Timpson P, Karim SA, Ridgway RA, Athineos D, Doyle B, et al. Mutant p53 drives metastasis and overcomes growth arrest/senescence in pancreatic cancer. Proceedings of the National Academy of Sciences of the United States of America. 2010;107(1):246-51.
11. Olive KP, Tuveson DA. The use of targeted mouse models for preclinical testing of novel cancer therapeutics. Clin Cancer Res. 2006;12(18):5277-87.
12. Siegel RL, Miller KD, Jemal A. Cancer statistics, 2020. CA Cancer J Clin. 2020;70(1):7-30.
13. Klein AP. Genetic susceptibility to pancreatic cancer. Mol Carcinog. 2012;51(1):14-24.
14. Hruban RH, Goggins M, Parsons J, Kern SE. Progression model for pancreatic cancer. Clin Cancer Res. 2000;6(8):2969-72.
15. Yachida S, Iacobuzio-Donahue CA. Evolution and dynamics of pancreatic cancer progression. Oncogene. 2013;32(45):5253-60.
16. Bardeesy N, DePinho RA. Pancreatic cancer biology and genetics. Nat Rev Cancer. 2002;2(12):897-909.

Table 1. Oncopig weights

Ad-K8-Cre dose (pfu)	Survival post-induction	Mean weight (Kg)				
		T_0	2 wk	4 wk	6 wk	Necropsy (8wk)
10^7	8 wk	27.5	26.8	34.5	38.8	45.8
10^8	8 wk	25.5	25.3	28.3	35.5	40.3
10^9	8 wk	20.0	25.8	27.5	27.0	28.5
10^10	8 wk	24.3	28.8	34.3	38.0	48.1
	p value	0.5	0.8	0.6	0.6	0.3

Table 2. Oncopig laboratory testing.

Ad-K8-Cre dose (pfu)	Sex	HG		HCT		AMYLASE		LIPASE		CEA		CA 19-9		AFP	
		T0	Necropsy	T0	Necropsy	T0	Necropsy	T0	Necropsy	T0	Necropsy	T0	Necropsy	T0	Necropsy
10^9	M	NA	8.5	NA	30	NA	669	NA	3	NA	0.1	NA	1	NA	0.5
	F	9.7	9.2	34.9	33	1520	1388	19	18	0.1	0.1	1	1	0.5	0.5
10^8	M	11	11.1	39.3	38.6	1015	1095	4	3	0.1	0.1	1	1	0.5	2.5
	F	11	9.4	40.3	33.6	1452	1749	27	3	0.1	0.1	1	1.4	0.8	1
10^7	M	9.3	10.6	32.9	37.3	573	739	8	21	0.1	0.1	2	1	0.5	1
	F	10.3	10.4	36.4	36.9	1551	1865	4	6	0.1	0.5	1	1	0.5	0.5
10^10	M	9.1	clotted	34.2	clotted	674	799	3	3	0.1	0.3	1	1	0.5	0.5
	F	10.4	10.2	38.2	36.9	1477	2556	3	3	0.1	0.1	1	1	0.5	0.5

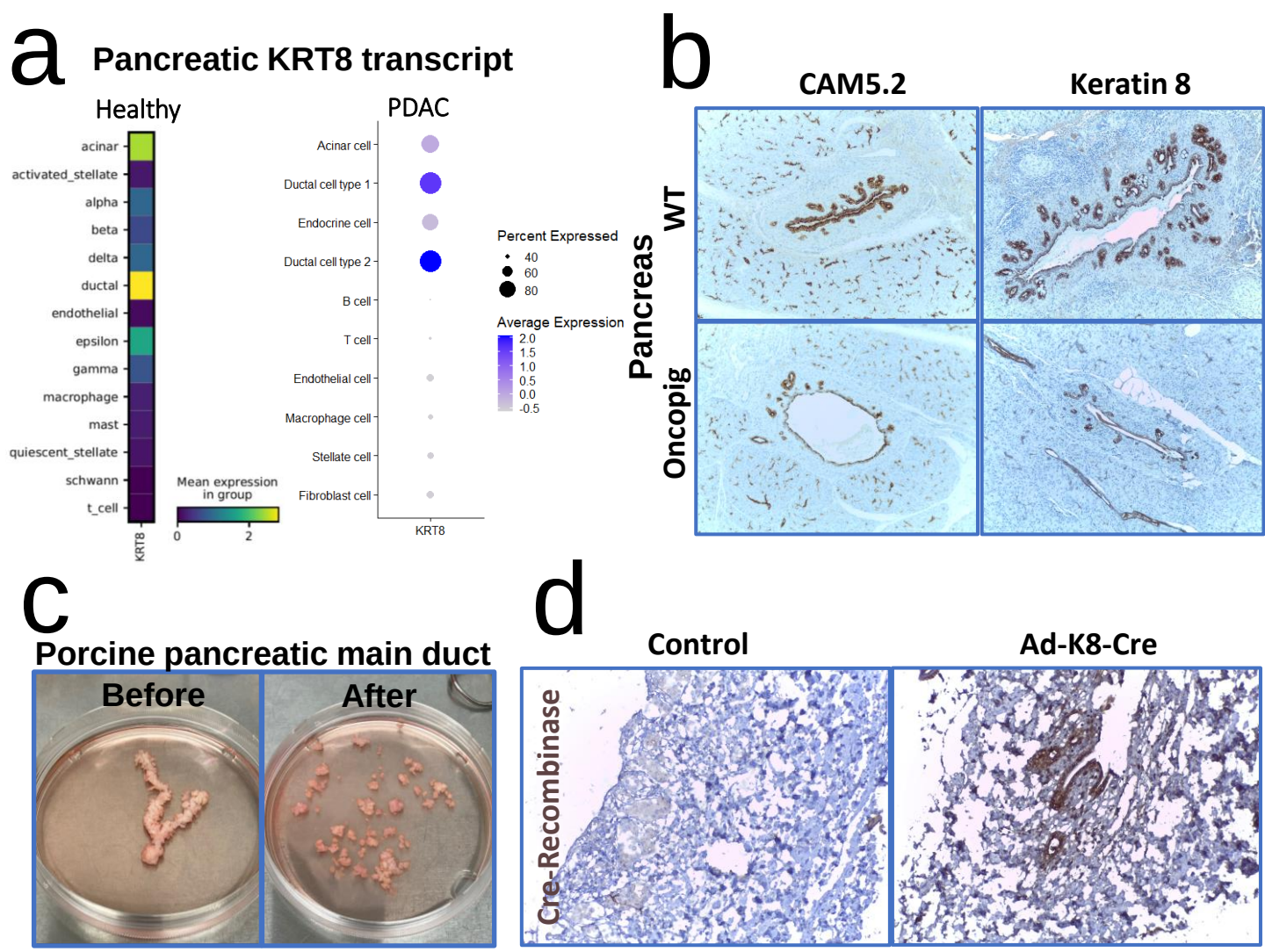
a
Pancreatic KRT8 transcript
Healthy
acinar
activated_stellate
alpha
beta
delta
ductal
endothelial
epsilon
gamma
macrophage
mast
quiescent_stellate
schwann
t_cell
KRT8
Mean expression in group
0
2
PDAC
Acinar cell
Ductal cell type 1
Endocrine cell
Ductal cell type 2
B cell
T cell
Endothelial cell
Macrophage cell
Stellate cell
Fibroblast cell
KRT8
Percent Expressed
40
60
80
Average Expression
2.0
1.5
1.0
0.5
0.0
-0.5
b
CAM5.2
Keratin 8
Pancreas
WT
Oncopig
c
Porcine pancreatic main duct
Before
After
d
Control
Ad-K8-Cre
Cre-Recombinase

Figure 1

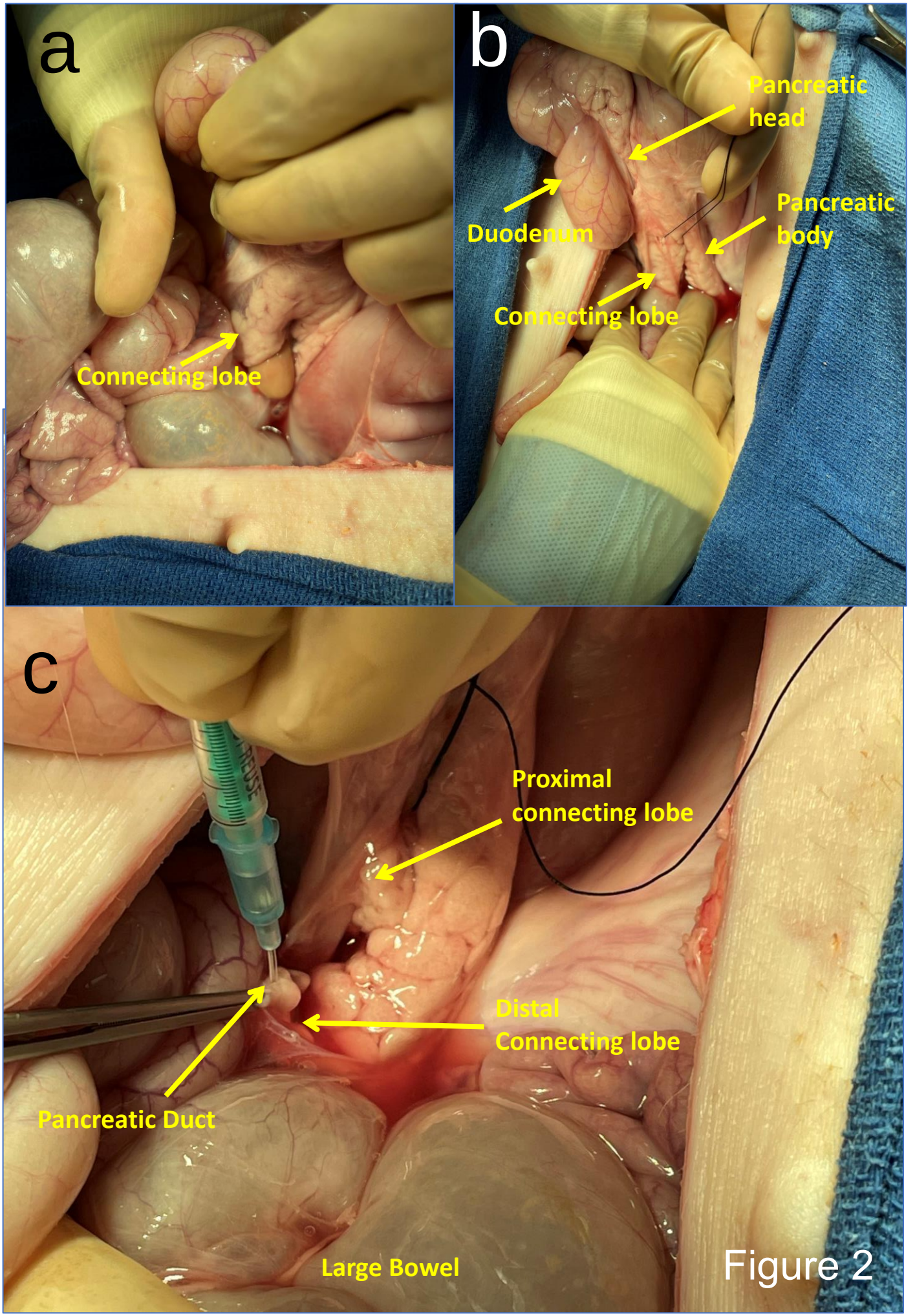
a
Connecting lobe
b
Pancreatic head
Duodenum
Pancreatic body
Connecting lobe
c
Proximal connecting lobe
Distal Connecting lobe
Pancreatic Duct
Large Bowel

Figure 2

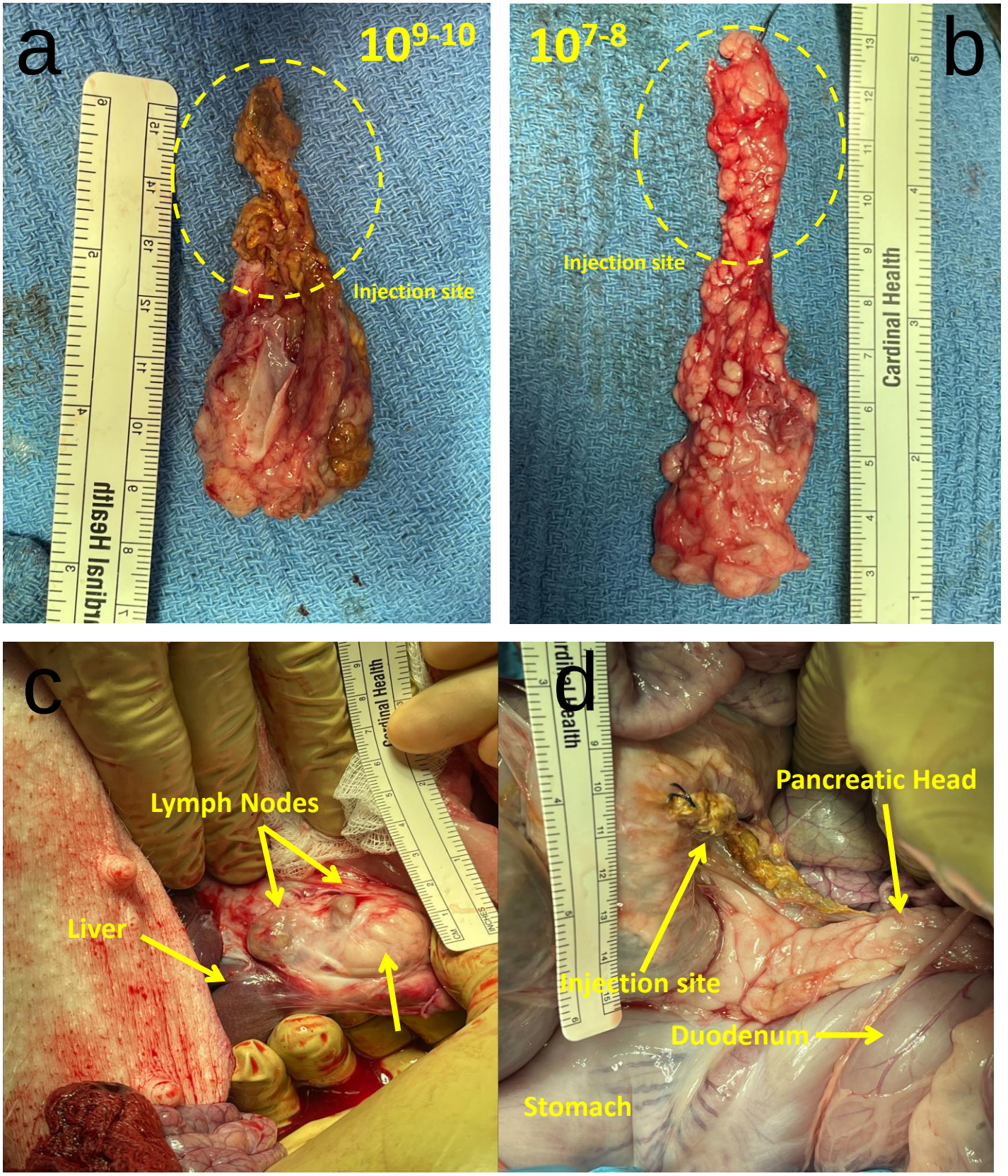
a
10^{9-10}
Injection site
b
10^{7-8}
Injection site
Cardinal Health
c
Lymph Nodes
Liver
d
Pancreatic Head
Injection site
Duodenum
Stomach

Figure 3

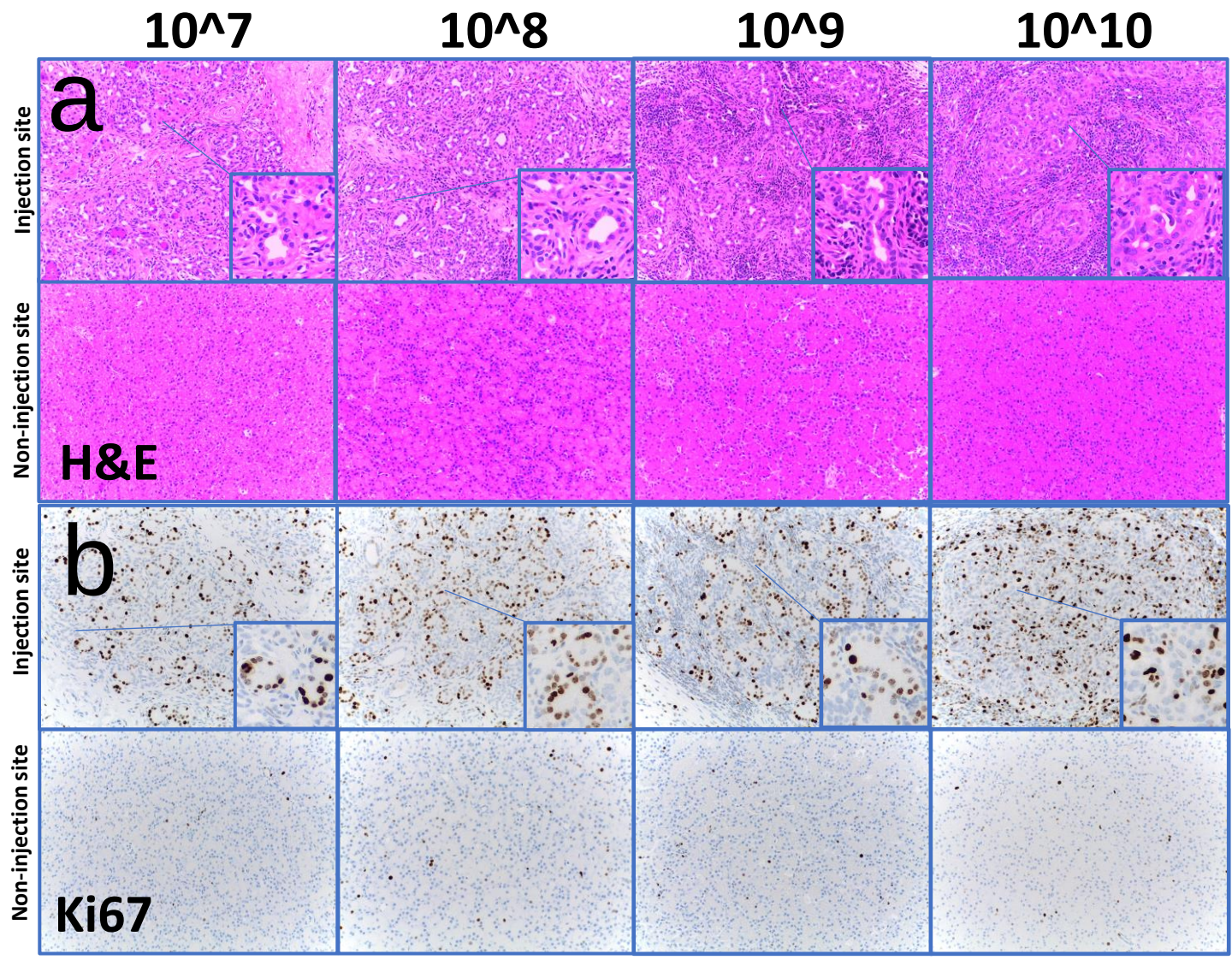
10^7
10^8
10^9
10^10
a
Injection site
Non-injection site
H&E
b
Injection site
Non-injection site
Ki67

Figure 4

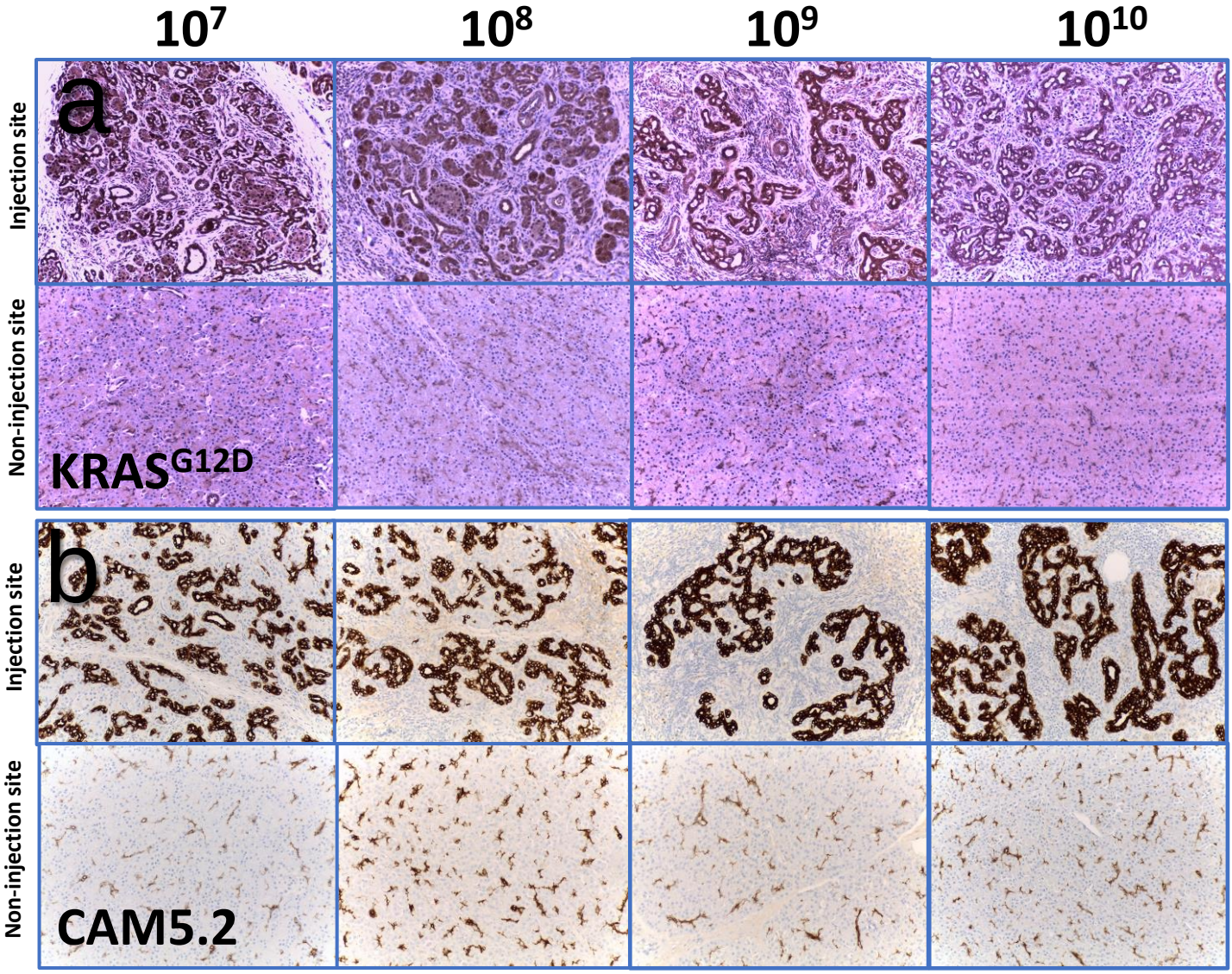
10^7
10^8
10^9
10^{10}
a
Injection site
Non-injection site
KRAS^{G12D}
b
Injection site
Non-injection site
CAM5.2

Figure 5

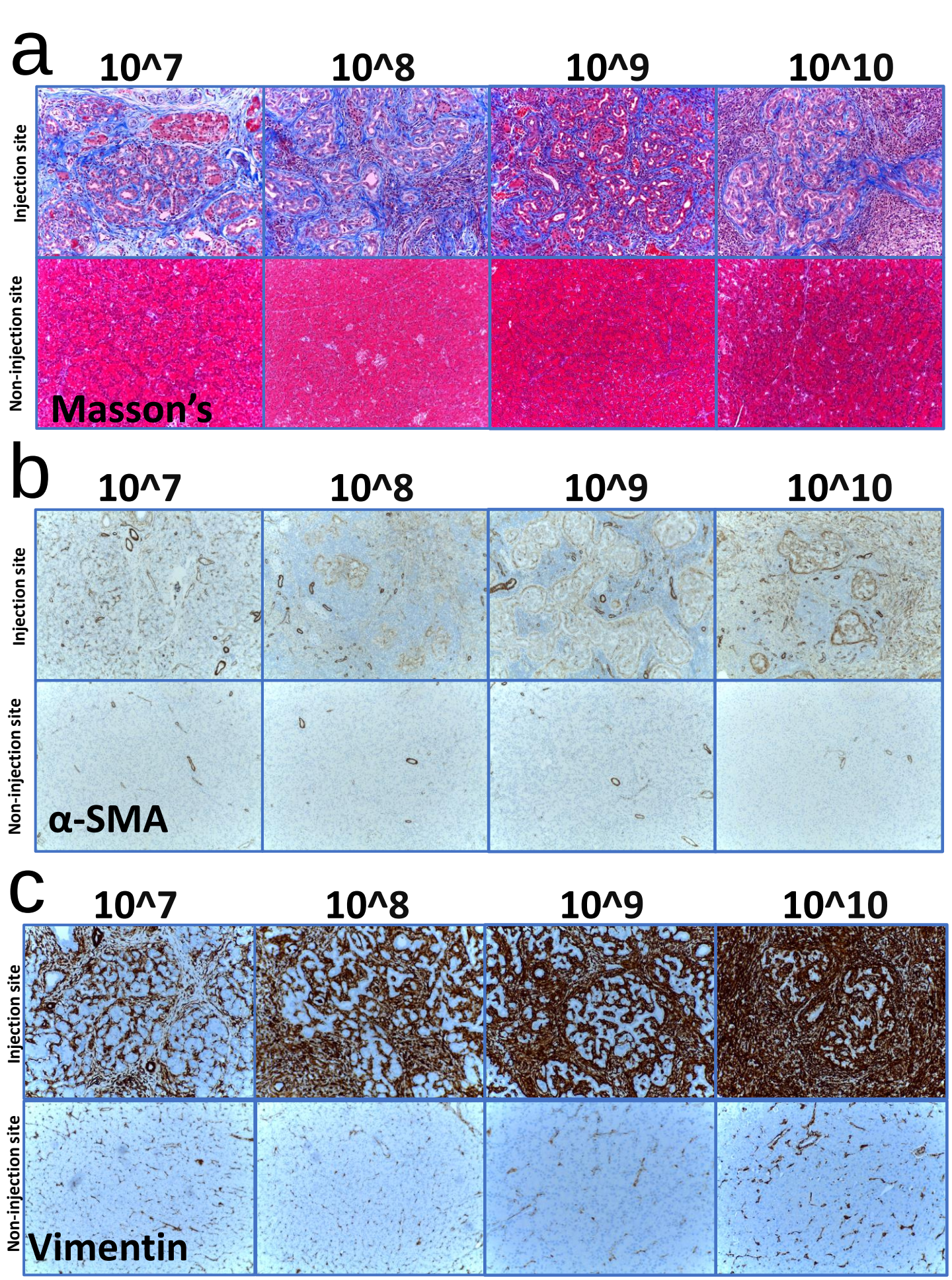
a
10^7
10^8
10^9
10^10
Injection site
Non-injection site
Masson's
b
10^7
10^8
10^9
10^10
Injection site
Non-injection site
α-SMA
c
10^7
10^8
10^9
10^10
Injection site
Non-injection site
Vimentin

Figure 6

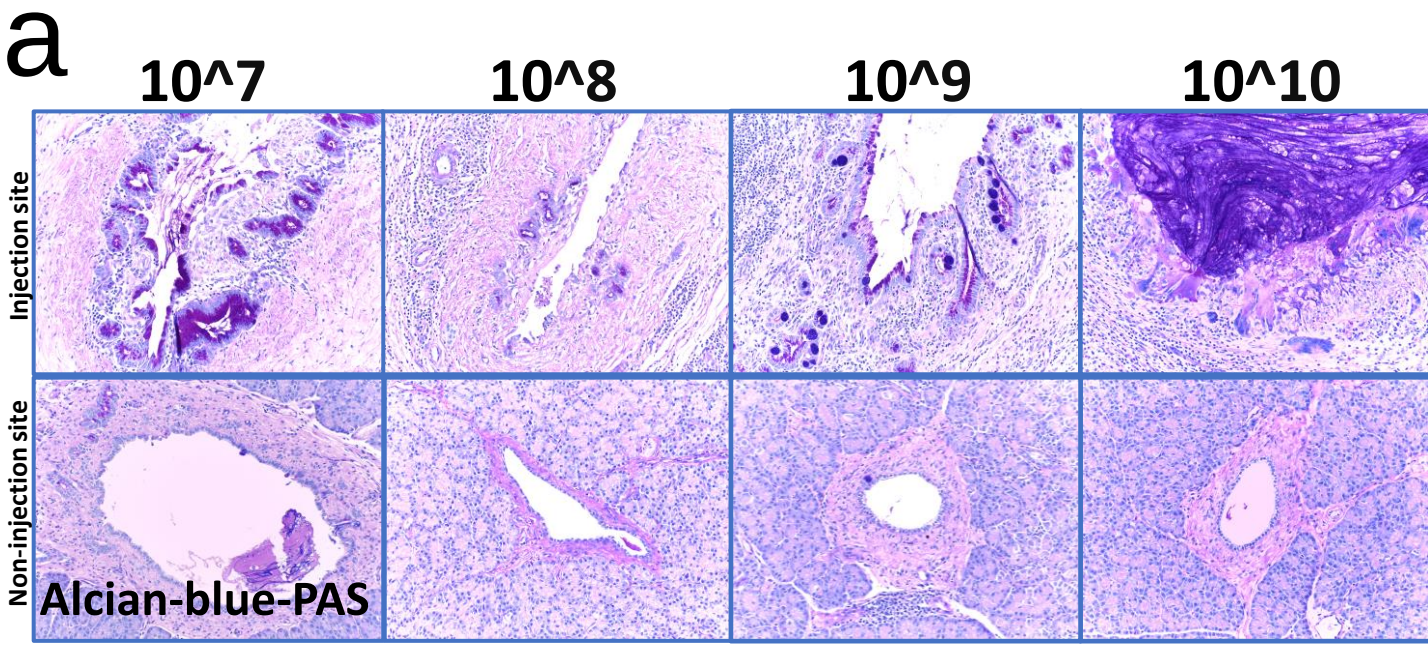
a
10^7
10^8
10^9
10^10
Injection site
Non-injection site
Alcian-blue-PAS

Figure 7

a

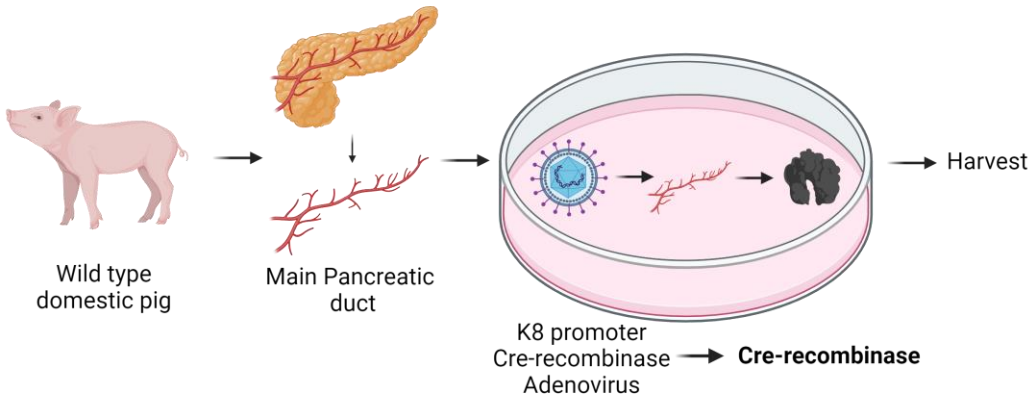

b

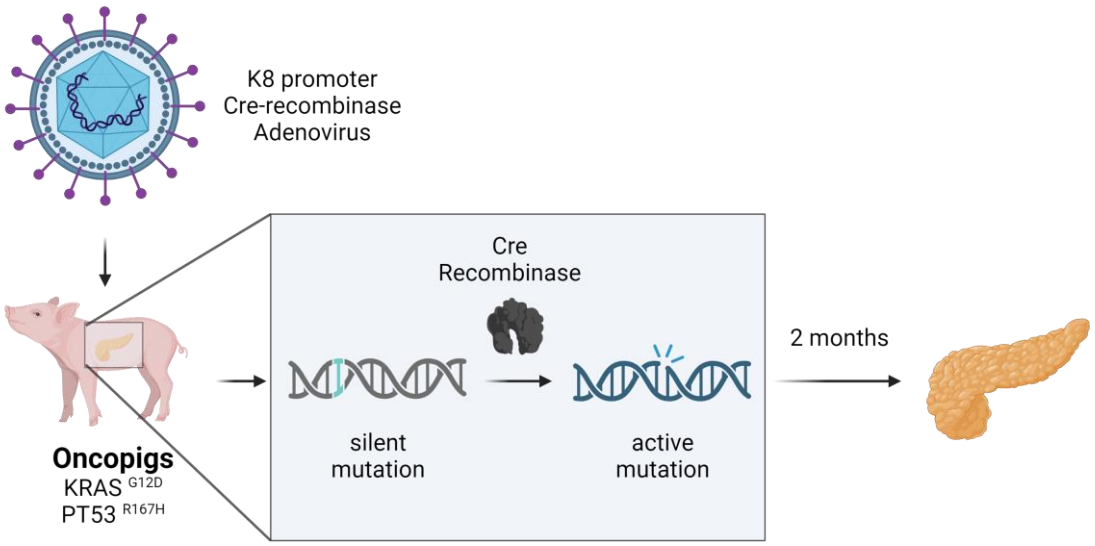

Supplementary Figure 1

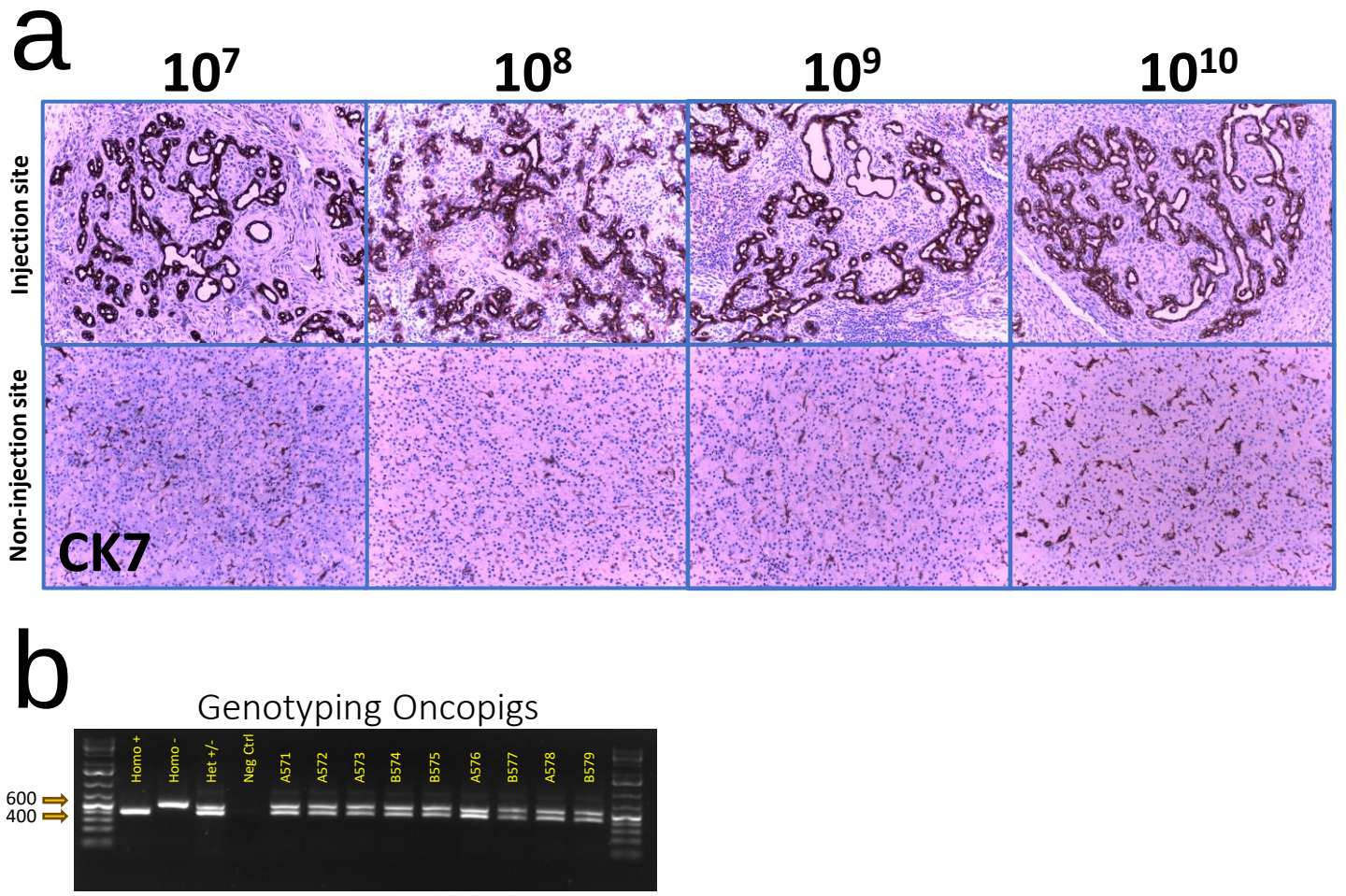

Supplementary Figure 2

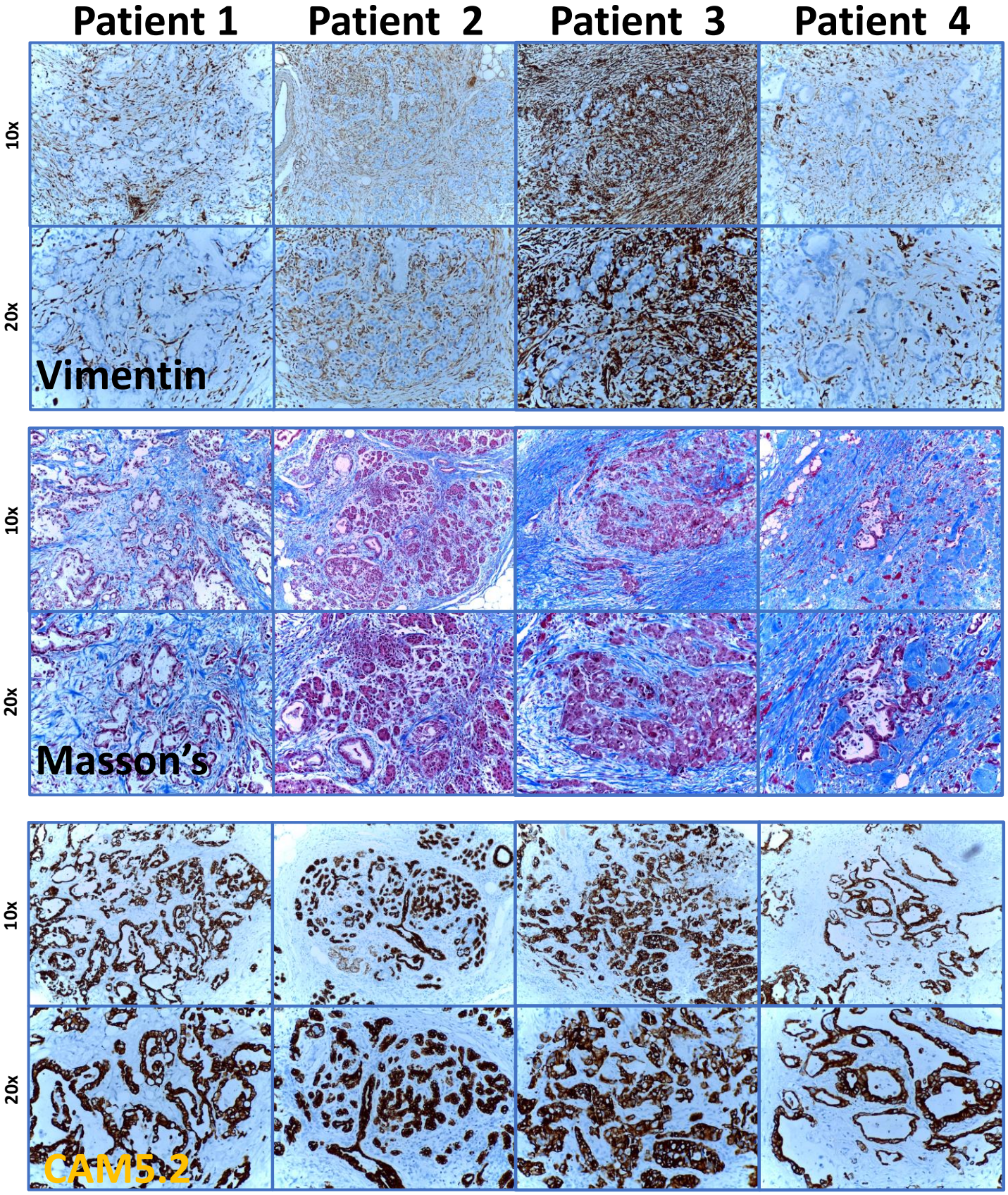

Supplementary Figure 3